

VRIQ: Benchmarking and Analyzing Visual-Reasoning IQ of VLMs

Tina Khezresmaeilzadeh¹ Jike Zhong¹ Konstantinos Psounis¹

Abstract

Recent progress in Vision Language Models (VLMs) has raised the question of whether they can reliably perform nonverbal reasoning. To this end, we introduce VRIQ (Visual Reasoning IQ), a novel benchmark designed to assess and analyze the visual reasoning ability of VLMs. We evaluate models on two sets of tasks: abstract puzzle-style and natural-image reasoning tasks. We find that on abstract puzzles, performance remains near random with an average accuracy of around 28%, while natural tasks yield better but still weak results with 45% accuracy. We also find that tool-augmented reasoning demonstrates only modest improvements. To uncover the source of this weakness, we introduce diagnostic probes targeting perception and reasoning. Our analysis demonstrates that around 56% of failures arise from perception alone, 43% from both perception and reasoning, and only a mere 1% from reasoning alone. This motivates us to design fine-grained diagnostic probe questions targeting specific perception categories (e.g., shape, count, position, 3D/depth), revealing that certain categories cause more failures than others. Our benchmark and analysis establish that current VLMs, even with visual reasoning tools, remain unreliable abstract reasoners, mostly due to perception limitations, and offer a principled basis for improving visual reasoning in multimodal systems.

1. Introduction

Recent years have witnessed remarkable advancements in both Large Language Models (LLMs) and Vision-Language Models (VLMs), transforming how artificial intelligence processes and understands multimodal information. These developments have been driven by novel architectures (Vaswani et al., 2017; Brown et al., 2020; Touvron et al., 2023), enhanced training methodologies (Chung et al., 2024;

¹University of Southern California, Los Angeles, USA. Correspondence to: Tina Khezresmaeilzadeh <khezresm@usc.edu>.

Ouyang et al., 2022), and massive-scale datasets (Schuhmann et al., 2022; Gadre et al., 2023). Reasoning capabilities have emerged as a cornerstone of LLM performance, with techniques such as chain-of-thought prompting (Wei et al., 2022), self-consistency (Wang et al., 2023a), and tree-of-thoughts (Yao et al., 2023) demonstrating that systematic reasoning dramatically improves performance on complex tasks. These reasoning approaches enable models to decompose problems, maintain logical consistency, and arrive at more accurate conclusions compared to direct answer generation, particularly benefiting mathematical problem-solving, logical deduction, and multi-step planning tasks.

In the visual domain, visual reasoning has become a focus of attention as researchers seek to extend these reasoning benefits to multimodal contexts. Visual reasoning—the ability to analyze, interpret, and draw logical conclusions from visual information—has become increasingly critical given VLMs’ deployment in high-stakes applications, including medical diagnosis (Li et al., 2023; Phan et al., 2024), and autonomous navigation (Pan et al., 2024; Chen et al., 2024). Recent efforts have introduced various approaches to enhance visual reasoning in VLMs, including visual chain-of-thought methods (Shao et al., 2024), tool-augmented reasoning systems (Gupta & Kembhavi, 2023; Surís et al., 2023), and reasoning-optimized models like OpenAI’s o3 and other specialized architectures (OpenAI, 2025e). However, despite these advances, recent evaluations have revealed persistent limitations in VLMs’ ability to perform complex visual reasoning tasks (Lu et al., 2024b; Yu et al., 2023), particularly when abstract thinking and multi-step inference are required.

To address these challenges, it is crucial to systematically evaluate current VLMs’ failure modes and identify specific areas requiring improvement. Several benchmarks have been proposed to assess visual reasoning capabilities (Li et al., 2024a; Jiang et al., 2024; Zhang et al., 2025a), yet they exhibit notable limitations. Some focus exclusively on natural image questions where reasoning requirements are relatively shallow and single-step (Fu et al., 2024a; Ging et al., 2024), while others concentrate solely on abstract reasoning tasks such as IQ-style puzzles without connecting to real-world visual understanding (Zhang et al., 2019; Barrett et al., 2018). Furthermore, existing benchmarks typically only evaluate perception and reasoning as monolithic ca-

pabilities (Cai et al., 2025). Here, perception refers to the ability to accurately identify visual elements (e.g., shapes, counts, positions), while reasoning is the subsequent process of applying abstract rules and principles to that perceived information to solve problems. Critically, no existing benchmark comprehensively evaluates: (1) how models perform on both natural and abstract visual questions using identical logical reasoning methodologies (such as odd-one-out problems), allowing direct comparison of model behavior across these domains, and (2) fine-grained diagnostic analysis identifying exact failure modes in specific perceptual and reasoning sub-capabilities, including color recognition, 3D/depth perception, counting, spatial positioning, rotation detection, and reasoning from textual descriptions versus actual images.

To investigate this gap, we present a comprehensive benchmark for evaluating visual reasoning in VLMs. Our benchmark comprises two parallel sets of questions—abstract image reasoning and natural image reasoning—organized under identical IQ test categories to enable direct comparison of model performance across visual domains. Questions are specifically designed to challenge VLMs’ capabilities across multiple dimensions. Additionally, we develop diagnostic probe questions for each IQ test, with each probe targeting specific aspects of perception or reasoning required to solve the main task. These probes, created through human annotation, enable us to dissect model failures systematically. Our analysis reveals three key insights: (i) both open source and proprietary models perform badly on the benchmark, even though it consists mostly of elementary school-grade IQ questions, see subsection 6.1, (ii) we quantify the distribution of errors across perception-only, reasoning-only, and combined perception-reasoning failures, and find that perception limitations are the main culprit, see subsection 6.2, and (iii) we measure the effect of different perception categories (counting, shape, color identification, position understanding, 3D/depth perception, etc.) on the visual reasoning abilities of VLMs and find that it differs sizably, see subsection 6.3. This benchmark and evaluation methodology for decomposing visual reasoning tasks facilitates precise failure detection and provides actionable insights for developing more capable models in both abstract and natural image reasoning. In summary, our contributions are:

1. A novel multidimensional visual reasoning benchmark consisting of five main IQ question categories containing both abstract and natural reasoning questions, enabling direct comparison of model performance across visual domains.
2. A hierarchical evaluation framework incorporating specific perception and reasoning probe questions to enable fine-grained diagnosis of model capabilities across sub-perceptual and reasoning tasks, revealing precise

failure modes.

3. Extensive experiments on a wide range of state-of-the-art VLMs, providing detailed insights into their strengths, weaknesses, and specific areas requiring improvement for advancing visual reasoning capabilities.

We plan to release the complete benchmark, all corresponding probing questions, and the methodology for constructing diagnostic probes for given images, facilitating community efforts toward developing more capable and reliable visual reasoning systems.

2. Related Work

Multimodal benchmarks. As the multimodal foundation model made significant progress in traditional vision tasks, it becomes increasingly important to develop an effective way of measuring their success. To achieve this, many general-purpose Visual Question Answering (VQA) tasks (Mathew et al., 2021; Gurari et al., 2018; Antol et al., 2015; Goyal et al., 2017; Singh et al., 2019; Hudson & Manning, 2019; Mathew et al., 2021; Marino et al., 2019; Li et al., 2024b; Liu et al., 2023; Liang et al., 2024; Saikh & et al., 2022; Yue et al., 2024b; Wang et al., 2023b; Chen et al., 2023) have been proposed. To provide a more focused evaluation for, many specialized benchmarks have been introduced: (Lu et al., 2024a; Zhang et al., 2024a; Qiao et al., 2024; Wang et al., 2024a; Lu et al., 2021; Li et al., 2025b; Wang et al., 2024c; Doris et al., 2024). Ours difference from them in that we specialize in puzzle and IQ problem solving and focus on analysis.

Solving multimodal IQ problems. Efforts have been made to evaluate VLMs on solving puzzle or IQ problems. Zhang et al. (2025b) focus on evaluating simple puzzle solving without symbolic or IQ questions. Li et al. (2025a) introduces more complex puzzle problem. MMIQ (Cai et al., 2025) is the closest to ours, which also evaluates multimodal performance on IQ problems; however, unlike MMIQ, our benchmark introduces both abstract and natural puzzle families in addition to a hierarchical probing framework, enabling fine-grained attribution of failures to different perceptual versus reasoning sources.

3. VRIQ: A Diagnostic Visual Reasoning Benchmark

We introduce VRIQ (Visual Reasoning IQ), a diagnostic benchmark of **N=1,500** expert-authored items that evaluates vision-language models on both perception and reasoning using IQ-style puzzles with multi-dimensional annotations. Unlike algorithmically generated datasets (e.g., PGM, RAVEN), VRIQ provides carefully constructed items anno-

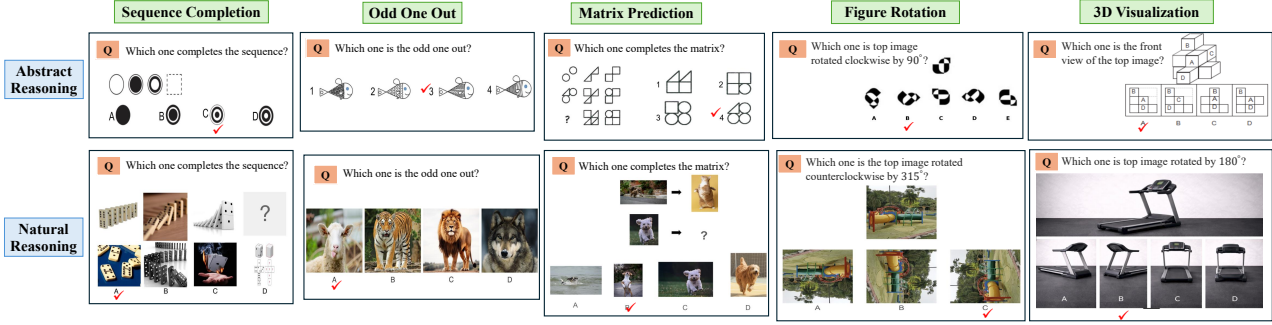


Figure 1. VRIQ Overview

tated with eight perceptual and five reasoning attributes, enabling reproducible error attribution and fine-grained failure-mode analysis.

3.1. Benchmark Design Principles

Parallel Domain Construction. VRIQ comprises two puzzle families—*abstract* and *natural*—that share identical reasoning categories and logical structures while differing only in visual domain. Each reasoning category (e.g., Sequence Completion, Matrix Prediction) is instantiated in both domains. Figure 1 presents representative paired examples across the five reasoning categories.

Abstract-domain puzzles. Abstract puzzles employ geometric primitives (shapes, lines, patterns) with multi-attribute transformations and high-similarity distractors. Items were constructed through two complementary avenues: (1) adaptation of publicly available **public-domain civil-service and aptitude examinations**, and (2) original designs created specifically for this benchmark. See Appendix C for details on source materials and modification strategies.

For the 3D Visualization category, we employ Tinkercad (Autodesk Inc., 2025), a web-based CAD platform, to generate precise geometric configurations and systematic viewpoint transformations.

Natural-domain puzzles. Natural puzzles were designed entirely in-house to preserve the same category-specific reasoning requirements while operating over real-world objects and scenes. For example, an Odd-One-Out task may require identifying functional or relational differences rather than geometric properties. More samples of natural-domain puzzles are provided in Appendix E.

Natural-domain examples were created using a human–AI collaborative pipeline. Human annotators first authored seed questions, which guided GPT-5.2-Thinking (OpenAI,

2025d) to propose task categories and problem instances. Images were obtained either via multimodal generation with GPT-5.2-Thinking or by manual sourcing from publicly available resources, depending on feasibility. Final examples were validated by human reviewers for logical consistency and visual clarity (see Appendix B).

VRIQ spans five fundamental reasoning categories established in human psychometrics: (1) Sequence Completion (SC), (2) Matrix Prediction (MP), (3) Odd One Out (OO), (4) Figure Rotation (FR), and (5) 3D Visualization (3D). For each category we generate **200** abstract-domain and **100** natural-domain puzzles, for a total of **1500** puzzles.

Quality Control. Human-annotated abstract items and expert-specified natural items were constructed using a unified multi-stage quality-control pipeline: all puzzles were independently solved by two annotators to verify answer correctness and uniqueness; all natural images were reviewed by at least two additional annotators to ensure rule consistency, visual clarity, and absence of artifacts or shortcut cues; and any failing items were regenerated or discarded. To reduce training-data contamination, adapted abstract items were systematically modified into novel instances and checked against common online repositories, while all natural-domain puzzles were created from original specifications rather than derived from existing datasets. This process yields high-fidelity, reproducible items with tightly controlled visual attributes and minimal risk of benchmark leakage.

4. Evaluation Framework

We evaluate VLMs on VRIQ using a diagnostic hierarchy intended to localize failures to (i) extracting task-relevant visual facts (*perception*) versus (ii) applying the underlying rule given those facts (*reasoning*).

4.1. Tier 1: End-to-End Accuracy

We first measure end-to-end multiple-choice accuracy across the five VRIQ categories: Sequence Completion (SC), Matrix Prediction (MP), Odd One Out (OO), Figure Rotation (FR), and 3D Visualization (3D). Each category contains both abstract and natural variants, enabling direct comparison across visual domains under matched task formats. Tier 1 reflects the combined effect of perception and reasoning.

4.2. Tier 2: Diagnostic Probes

To diagnose failures, we construct two probe types for each puzzle. **Perceptual probes (P-probes).** P-probes are atomic questions designed to test *one* task-relevant visual attribute at a time (e.g., count, color, relative position, orientation). They are asked with the original image and are designed to be human-trivial (e.g., “*How many red circles are shown?*”). **Reasoning probes (R-probes).** R-probes test whether the model can apply the same logical operation as the original puzzle when the relevant visual facts are provided explicitly in text. Concretely, for each puzzle we write a text-only instantiation of the rule (e.g., “each element rotates clockwise by 45°”) and specify the necessary facts (e.g., the observed rotations at positions 1–3), then ask for the implied missing outcome. R-probes therefore measure reasoning given explicit facts. Because they remove visual extraction, R-probe accuracy serves as an upper bound on end-to-end accuracy for the corresponding puzzle family under our probe design.

4.3. Tier 3: Error Categorization and Bounds

For each *failed* end-to-end puzzle, we evaluate the associated P- and R-probes and assign one of three diagnostic outcomes. **Perception bottleneck evidence (P-only):** A failure is labeled **P-only** if the model fails at least one P-probe but succeeds on the corresponding R-probe. This indicates that the model can apply the rule when given correct facts, but fails to extract at least one required fact from the image. This category provides a *lower bound* on perception-driven failures. **Reasoning deficit evidence (R-only):** A failure is labeled **R-only** if the model passes all P-probes but fails the corresponding R-probe. Under our probe set, this indicates that the model extracted the probed task-relevant facts but fails to apply the logical operation even when the same facts are provided explicitly. This category provides a *lower bound* on reasoning-driven failures. **Both failures (P+R):** A failure is labeled **P+R** if the model fails at least one P-probe and also fails the R-probe.

4.4. Multi-Dimensional Annotation Schema

Each puzzle is annotated along eight perceptual dimensions to ensure systematic coverage: Color, Shape, Count, Position, Rotation/Orientation, 3D/Depth, Symmetry/Pattern,

and Distractor Similarity. These dimensions were chosen based on recurring failure modes of VLMs documented in prior work (Rahmanzadehgervi et al., 2024; Kamath et al., 2023; Zhang et al., 2024b; Khemlani et al., 2025). Annotations ensure that each puzzle’s perceptual demands are explicit, and they enable alignment between probe design and puzzle requirements.

4.5. Probe Construction Protocol

For each puzzle, we generate probes corresponding only to the perceptual dimensions required to solve it. This avoids introducing irrelevant attributes and ensures diagnostic precision. Probes are designed to be trivial for humans, so any model failure can be unambiguously attributed to the intended dimension. See [Appendix A](#) for a detailed worked example of a matrix reasoning puzzle decomposed into perceptual and reasoning probes. This hierarchical design moves beyond aggregate accuracy to reveal whether failures are caused by perception, reasoning, or their interaction, providing actionable signals for model analysis and improvement.

5. Experimental Setup

We evaluate a diverse set of open-source and proprietary vision-language models (VLMs), chosen to span model scale, architecture, and reasoning capabilities:

Open-source models Qwen2.5-VL-3B-Instruct ([Huggingface, 2025b](#)), Qwen2.5-VL-3B-Instruct-AWQ (quantized) ([Huggingface, 2025c](#)), Qwen2.5-VL-7B-Instruct ([Huggingface, 2025d](#)), Qwen3-VL-32B-Thinking ([Bai et al., 2025](#)), InternVL3-9B ([Huggingface, 2025a](#)), llava-v1.6-mistral-7b-hf ([Huggingface, 2025f](#)), llava-v1.6-vicuna-7b-hf ([Huggingface, 2025g](#)) and llava-v1.6-34b-hf [Huggingface, 2025e](#). These models represent the widely used open community baselines, covering both instruction-tuned and quantized variants. We include them to assess how parameter count and efficiency trade-offs affect both perceptual and reasoning probes.

Frontier / proprietary models GPT-5.1 ([OpenAI, 2025c](#)), GPT-4o ([OpenAI, 2025a](#)), GPT-4o-mini ([OpenAI, 2025b](#)), Gemini-2.5-pro ([Comanici et al., 2025](#)), OpenAI o3 (“thinking with images”) ([OpenAI, 2025e](#)). These API-served models are larger and trained with broader multimodal pre-training pipelines. GPT-4o and GPT-4o-mini are optimized for image-text interaction, while o3 is explicitly designed for reasoning with tool use.

Special Case: o3 and Tool-Enhanced Reasoning. We evaluate OpenAI o3 via the official OpenAI API in its “thinking with images” mode ([OpenAI, 2025f](#)), which enables

the model to invoke visual manipulation and computation tools during inference. In our evaluation, o3 is allowed to use (i) image cropping, (ii) zoom/magnification, (iii) image rotation, and (iv) Python code execution for lightweight quantitative checks. To ensure a controlled and reproducible setting, we use deterministic decoding (temperature = 0) and cap tool usage to at most 10 tool calls per question. We include o3 to test whether tool-augmented inference mitigates perceptual bottlenecks (e.g., rotation, counting, and spatial localization) identified by our diagnostic probes. This provides insight into how tool-enhanced multimodal systems can extend beyond traditional VLM capabilities.

Human baseline. We evaluate human performance on a stratified subset of 300 questions, sampling 30 questions from each (category \times domain) cell (5 categories \times 2 domains). We recruit 20 participants (ages 18–55, mixed academic backgrounds). Each participant solves 30 questions, and each question is independently answered by two annotators. Participants are not subject to time limits and are instructed to prioritize accuracy over speed. We report mean human accuracy with 95% confidence intervals.

6. Results

In this section, we summarize our key results from evaluation on VRIQ using the models mentioned in section 5. The results for abstract questions are displayed in Table 1 and their natural variants are shown in Table 2. We also include a random guess baseline for reference.

6.1. Main results

VLMs fail at abstract IQ questions—even proprietary ones. We observed that across all categories, VLMs show overall poor performance. Among all models tested¹, Qwen3-VL-32B-Thinking shows the best performance, scoring an average of **35.5%** across all categories, which is only **10.5%** above the random guess baseline.

Overall, when averaged among all VLMs tested, the improvement compared to random guess is only about **2.52%** (27.52% vs. 25%), despite these problems being easily solvable by humans. Surprisingly, our results show that **even proprietary VLMs do not show much better performance** on abstract IQ questions. For example, gpt-4o (Hurst & OpenAI, 2024) and gpt-4o-mini achieve average accuracies of only **30.3%** and **25.1%**, respectively, and do not consistently outperform strong open-source models such as Qwen3-VL-32B-Thinking and Qwen2.5-VL-7B-Instruct.

¹Note that this excludes gpt-o3 with “thinking with image” as it belongs to a different model family and can leverage external tools. We further analyze the details of its improvement in section 7

This observation diverges from prior work which finds proprietary VLMs to perform considerably better than open-sourced ones (Yue et al., 2024a; 2025; Fu et al., 2024b; Li et al., 2025b; Wang et al., 2024b; Lu et al., 2024c). **This suggests that scaling model sizes and training data is not enough to address the perception limitations of models**, as we discuss in detail in subsection 6.2. More importantly, we note that the abstract IQ questions in our benchmark can all be found in a myriad of decades-old IQ tests regularly used to assess human IQ across a wide range of ages; failure on these problems reveals a particular and critical deficiency in tackling abstract symbolic problems even with state-of-the-art multimodal foundation models. We conduct in-depth analysis over the errors in section 7 and show that surprisingly, most of the errors come from perception rather than reasoning. In addition, we observe that performance varies substantially across categories and models, indicating that our benchmark meaningfully distinguishes different model behaviors even under a fixed question format. Human annotators achieve an average accuracy of 90.36% (95% CI: [89.11%, 91.61%]) on the evaluated subset of 300 questions in the abstract domain, and 98.20% (95% CI: [97.66%, 98.75%]) in the natural domain, substantially outperforming all tested VLMs in both settings.

Different models exhibit different strengths. Although the overall accuracy of each model is relatively poor, closer inspection reveals substantial variance across categories (Table 1, Table 2). This variance indicates that current VLMs do not fail uniformly but instead display heterogeneous strengths and weaknesses.

For example, on matrix prediction (MP), Qwen3-VL-32B-Thinking achieves the highest accuracy among standalone models (34%), followed by Qwen2.5-VL-7B-Instruct and InternVL3-9B (both 31%), while several other models remain near or below 20%. Conversely, Qwen2.5-VL-3B-Instruct-AWQ reaches **30%** on 3D reasoning but drops to **20%** on odd-one-out (OO).

This cross-category divergence is not limited to open-source models: surprisingly, the GPT-4o family, despite its scale and proprietary training, does not dominate in any single category and often trails behind smaller open-source alternatives.

Such patterns underscore an important observation: *while no model excels universally, each exhibits localized competence in specific problem types*. This specialization suggests that architectural or training differences—such as alignment objectives, quantization, or reliance on language priors—may selectively benefit certain categories while hindering others. The practical implication is that model choice should depend strongly on the target task distribution, as relying

Table 1. Accuracy (%) of different vision–language models (VLMs) on the VRIQ benchmark across five categories: SC = Sequence Completion, 3D = 3D Reasoning, FR = Figure Rotation, OO = Odd One Out, and MP = Matrix Prediction.

Model	SC (%)	3D (%)	FR (%)	OO (%)	MP (%)	Avg (%)
Random Guess	25	25	25	25	25	25
Open Source VLMs						
Qwen2.5-VL-3B-Instruct	20.5	28	23	25.5	17	22.8
Qwen2.5-VL-3B-Instruct-AWQ	20.5	30	17	20	19.5	21.4
Qwen2.5-VL-7B-Instruct	40.5	33	25	26.5	31	31.2
Qwen3-VL-32B-Thinking	44.5	34	31.5	33.5	34	35.5
InternVL3-9B	24	32	20	16.5	31	24.7
llava-v1.6-mistral-7b-hf	16	28.5	20	27	20	22.3
llava-v1.6-vicuna-7b-hf	23.5	24	16	15	18.5	19.4
llava-v1.6-34b-hf	25	23	20	20	26	22.8
Proprietary VLMs						
gpt-5.1	28	27	31	33.5	27	29.3
gpt-4o	28.5	31	32	30.5	29.5	30.3
gemini-2.5-pro	27	29.5	31.5	27.5	28	28.7
gpt-5-mini	24.5	22	24	26	11.5	21.6
gpt-4o-mini	23.5	25	25	28.5	23.5	25.1
gpt-o3 (thinking with image)	48.5	35	68	52.5	47	50.2
Avg %	28.18	28.71	27.43	27.32	25.96	27.52
Human Baseline %	93.43	85.82	92.54	90.92	89.09	90.36

on a single “state-of-the-art” model may be insufficient for broad-spectrum reasoning.

VLMs perform better on natural variants, but remain unreliable. The natural variants of our IQ benchmark reveal a markedly different trend compared to their abstract counterparts (Table 2). Whereas abstract reasoning tasks reduce most models to near-chance accuracy, grounding the problems in natural imagery leads to consistent gains of roughly 10–20 percentage points above random guess across nearly all categories. For example, average performance on sequence completion improves from **28.18%** in the abstract setting to **44.21%** in the natural setting, and on odd-one-out from **27.32%** to **47.29%**. These improvements demonstrate that perceptual grounding substantially reduces task difficulty. This is reasonable since these models are mainly trained on natural-image-based QA data rather than symbolic patterns. Crucially, it supports our hypothesis that many errors observed in abstract settings arise not purely from reasoning deficits but from failures of low-level visual perception.

Despite this encouraging trend, reliability remains limited. Even in the natural setting, performance is far from human-level: the best open-source models cluster around **35%–47%**, while proprietary models such as GPT-4o achieve an average of **54.2%**. Moreover, variance across categories and models remains striking. For instance, llava-v1.6-vicuna-7b-hf attains **19%** on 3D reasoning

but only **24%** on sequence completion, reflecting an inconsistency that precludes dependable deployment.

This heterogeneity suggests that gains from natural grounding are unevenly distributed across categories and architectures, indicating that current models do not acquire a generalizable “IQ-like” competence but rather exploit superficial cues available in specific tasks. We provide more detailed studies in subsection 6.3.

Using tools to “think with image” largely improves performance. Across both abstract and natural variants, although most models show poor performance, we observe a substantial leap with gpt-o3 (tool-augmented) (OpenAI, 2025). Unlike other gpt series models such as gpt-4o or gpt-4o-mini, gpt-o3 is equipped with external tool use, allowing the model to apply Python-coded operations such as “cropping,” “magnification,” and “distortion.” These operations enable the model to actively manipulate the input image, thereby enhancing visual perception by focusing on the most relevant regions and reducing hallucinations.

On the abstract benchmark, gpt-o3 achieves **48.5%** on sequence completion and **68%** on figure rotation, compared to near-random performance ($\sim 25\%$) by all other models. On the natural benchmark, the gains are even more striking: it reaches **80%** on sequence completion, **70%** on odd-one-out, and **100%** on 3D reasoning and **92%** on figure rotation—often more than doubling the accuracy of the strongest baseline. This makes gpt-o3 the only model in

Table 2. Accuracy on natural reasoning categories. FR questions are 3-choice questions.

Model	SC (%)	OO (%)	FR (%)	3D (%)	MP (%)	Avg (%)
Random Guess	25	25	33	25	25	26.6
Open Source VLMs						
Qwen2.5-VL-3B-Instruct	34	41	40	30	43	37.6
Qwen2.5-VL-3B-Instruct-AWQ	37	36	35	25	29	32.4
Qwen2.5-VL-7B-Instruct	25	50	35	0	40	30
Qwen3-VL-32B-Thinking	42	54	49	41	50	47.2
InternVL3-9B	40	40	45	40	35	40
llava-v1.6-mistral-7b-hf	20	30	0	27	25	20.4
llava-v1.6-vicuna-7b-hf	24	34	15	19	15	21.4
llava-v1.6-34b-hf	40	44	20	27	43	34.8
Proprietary VLMs						
gpt-5.1	59	60	40	41	59	51.8
gpt-4o	64	57	40	48	62	54.2
gemini-2.5-pro	61	50	33	59	65	53.6
gpt-5-mini	49	48	40	28	51	43.2
gpt-4o-mini	44	48	40	39	48	43.8
gpt-o3 (thinking with image)	80	70	92	100	75	85.0
Avg %	44.21	47.29	38.00	37.43	45.71	42.53
Human Baseline %	98.77	98.83	98.84	97.22	97.35	98.2

Table 3. Perception vs. reasoning error distribution. Percentage of failures attributed to perception-only, reasoning-only, and combined failures across five VLMs.

Model	P-only (%)	R-only (%)	P+R (%)
4o mini	56.36	0.00	43.64
4o	60.00	3.64	36.36
Q3BAWQ	56.36	0.00	43.64
Qwen3B	52.73	1.82	43.64
Qwen-7B	52.73	0.00	47.27
Avg (%)	55.84	1.10	43.07

our study to approach human-like competence on certain tasks. Gemini-2.5-pro closely matches GPT-4o in the natural domain (53.6% vs. 54.2%) but remains similarly weak in the abstract setting (28.7%).

Qualitative Analysis of Tool Usage. To understand how tool augmentation improves performance, we analyze o3’s logged tool-call traces on a stratified sample of 50 questions (10 per category). We observe that o3 most frequently uses cropping and zooming to isolate small visual elements prior to answering, and uses rotation to canonicalize orientation in figure-rotation and 3D-view questions. In a subset of cases, o3 also invokes Python for simple quantitative checks (e.g., counting elements in a cropped region or finding the position of a shape in a region). Representative tool-call examples are provided in Appendix D.

These findings suggest that current MLLM limitations on IQ-style reasoning are driven not only by model architecture but also by the lack of interactive perception mechanisms. While gpt-o3 illustrates the potential of tool-augmented reasoning, it also reveals a widening gap between standalone models and systems embedded in tool-use pipelines, indicating that complex multimodal reasoning may rely more on orchestrating external procedures than on further scaling single models.

6.2. Perception versus reasoning

To understand the root causes behind poor performance on abstract IQ tasks, we conducted fine-grained diagnostic analysis using our hierarchical probe methodology on five representative models: ChatGPT-4o-mini, ChatGPT-4o, Qwen2.5-VL-3B-Instruct-AWQ, Qwen2.5-VL-3B-Instruct, and Qwen2.5-VL-7B-Instruct. Human annotators classified each failure as perception-only, reasoning-only, or combined perception-reasoning error. Table 3 reveals a striking pattern: perception errors dominate across all models, accounting for 55.4% of failures on average, while reasoning-only errors represent just 1.1%—a 50:1 ratio that holds remarkably consistent regardless of model scale or architecture.

The near-absence of pure reasoning failures (0-3.64% across models) indicates that when visual elements are correctly perceived, models reliably apply appropriate logical operations. The substantial “Both” category (36.4-47.3%) likely

Table 4. Detailed perception probe failure rates. Failure rates (%) for each probe type across IQ categories, with averages reported in the final column. N/A indicates probes not applicable to a given task category.

Probe Type	SC (%)	MP (%)	OO (%)	FR (%)	3D (%)	Avg (%)
Color	26.67	47.50	20.00	N/A	N/A	31.39
Shape	35.68	60.00	65.00	80.00	N/A	60.17
Count	64.29	80.00	77.50	75.00	72.21	73.80
Position	56.22	73.33	50.00	51.43	60.00	58.20
Rotation/Orientation	45.39	50.00	50.00	64.00	N/A	52.35
3D/Depth	N/A	N/A	N/A	70.00	65.00	67.5
Symmetry/Pattern	40.91	46.67	75.00	N/A	N/A	54.19
Distractor Similarity	52.00	N/A	46.33	N/A	N/A	49.17

represents perception errors cascading into apparent reasoning mistakes rather than independent dual failures, given the rarity of isolated reasoning errors.

These results fundamentally challenge assumptions about abstract visual reasoning requirements. **Rather than needing more sophisticated reasoning mechanisms, models face an almost entirely perceptual bottleneck—struggling to extract visual information accurately** rather than to apply logical operations to that information.

6.3. Fine-Grained Probe Analysis.

To diagnose perception bottlenecks in more detail, Table 4 reports probe-level failure rates across categories, averaged over five VLMs. Some probe types are marked N/A, as they were not relevant for specific IQ categories (e.g., 3D/Depth was not designed into Sequence Completion). This confirms that our diagnostic design is targeted: probes reflect only the perceptual attributes actually needed for solving each category. A clear pattern emerges: certain perceptual categories exhibit consistently high failure rates. Counting (73.8%), position (58.2%), and rotation/orientation (52.4%) show systematic weaknesses across models and categories. These attributes require precise spatial encoding and robust relational perception, where even minor visual noise cascades into reasoning errors. By contrast, color shows substantially lower failure rates (31.4%), suggesting that models’ visual backbones are better tuned for appearance-based attributes than for spatial or quantitative ones—likely reflecting dataset biases toward object-level recognition rather than relational structure.

Errors in 3D/Depth (67.5%) and symmetry/pattern (54.2%) further demonstrate that VLMs lack strong 3D geometric priors and abstract relational sensitivity. Together, these probe results confirm that perception failures are not monolithic, but span multiple subtypes with distinct difficulty profiles, underscoring the need for perception-focused improvements to unlock more reliable reasoning.

7. Discussion and Limitations

Implications for Model Development. Together, these findings suggest that advancing VLM reasoning requires targeted improvements to perceptual grounding rather than simply scaling reasoning capacity. Enhancing spatial and quantitative perception—through stronger geometric priors, explicit counting mechanisms, or training data emphasizing relational structure—may yield more reliable reasoning than purely architectural tweaks to attention or prompting. Furthermore, evaluation benchmarks should explicitly disentangle perception from reasoning to avoid conflating perceptual noise with logical inference.

Limitations. While VRIQ provides a principled diagnostic framework for visual reasoning, our focus on static IQ-style puzzles limits scope. Dynamic reasoning tasks—temporal prediction, causal inference in video, or embodied navigation—may reveal different failure patterns. Our probe set targets core visual primitives (count, position, rotation); extending to higher-level attributes (texture, affordances) could uncover additional bottlenecks. Future work should test whether the perception-reasoning hierarchy generalizes to richer domains like chart understanding, scientific diagrams, and multimodal documents.

8. Conclusion

We introduced VRIQ, a diagnostic benchmark that isolates perceptual and reasoning failures in VLMs. Our analysis reveals that perception—particularly in counting, spatial localization, and orientation—is the primary bottleneck, while pure reasoning errors are rare. These results suggest that advancing VLM performance requires prioritizing perceptual grounding over architectural scaling. By shifting from descriptive to diagnostic evaluation, VRIQ provides a principled framework for developing more robust multimodal models.

References

Antol, S., Agrawal, A., Lu, J., Mitchell, M., Batra, D., Zitnick, C. L., and Parikh, D. Vqa: Visual question answering. In *Proceedings of the IEEE International Conference on Computer Vision (ICCV)*, pp. 2425–2433, 2015.

Autodesk Inc. Tinkercad. <https://www.tinkercad.com>, 2025. Accessed: 2026-01-05.

Bai, S., Cai, Y., Chen, R., Chen, K., Chen, X., Cheng, Z., Deng, L., Ding, W., Gao, C., Ge, C., Ge, W., Guo, Z., Huang, Q., Huang, J., Huang, F., Hui, B., Jiang, S., Li, Z., Li, M., Li, M., Li, K., Lin, Z., Lin, J., Liu, X., Liu, J., Liu, C., Liu, Y., Liu, D., Liu, S., Lu, D., Luo, R., Lv, C., Men, R., Meng, L., Ren, X., Ren, X., Song, S., Sun, Y., Tang, J., Tu, J., Wan, J., Wang, P., Wang, P., Wang, Q., Wang, Y., Xie, T., Xu, Y., Xu, H., Xu, J., Yang, Z., Yang, M., Yang, J., Yang, A., Yu, B., Zhang, F., Zhang, H., Zhang, X., Zheng, B., Zhong, H., Zhou, J., Zhou, F., Zhou, J., Zhu, Y., and Zhu, K. Qwen3-vl technical report, 2025. URL <https://arxiv.org/abs/2511.21631>.

Barrett, D., Hill, F., Santoro, A., Morcos, A., and Lillicrap, T. Measuring abstract reasoning in neural networks. In *International conference on machine learning*, pp. 511–520. PMLR, 2018.

Brown, T., Mann, B., Ryder, N., Subbiah, M., Kaplan, J. D., Dhariwal, P., Neelakantan, A., Shyam, P., Sastry, G., Askell, A., Agarwal, S., Herbert-Voss, A., Krueger, G., Henighan, T., Child, R., Ramesh, A., Ziegler, D., Wu, J., Winter, C., Hesse, C., Chen, M., Sigler, E., Litwin, M., Gray, S., Chess, B., Clark, J., Berner, C., McCandlish, S., Radford, A., Sutskever, I., and Amodei, D. Language models are few-shot learners. In Larochelle, H., Ranzato, M., Hadsell, R., Balcan, M., and Lin, H. (eds.), *Advances in Neural Information Processing Systems*, volume 33, pp. 1877–1901. Curran Associates, Inc., 2020. URL https://proceedings.neurips.cc/paper_files/paper/2020/file/1457c0d6bfcb4967418bfb8ac142f64a-Paper.pdf.

Cai, H., Yang, Y., and Hu, W. Mm-iq: Benchmarking human-like abstraction and reasoning in multimodal models. *arXiv preprint arXiv:2502.00698*, 2025.

Chen, S. et al. TheoremQA: A theorem-driven question answering dataset. *arXiv preprint arXiv:2305.12524*, 2023.

Chen, Y., Ding, Z.-h., Wang, Z., Wang, Y., Zhang, L., and Liu, S. Asynchronous large language model enhanced planner for autonomous driving. In *European Conference on Computer Vision*, pp. 22–38. Springer, 2024.

Chung, H. W., Hou, L., Longpre, S., Zoph, B., Tay, Y., Fedus, W., Li, Y., Wang, X., Dehghani, M., Brahma, S., Webson, A., Gu, S. S., Dai, Z., Suzgun, M., Chen, X., Chowdhery, A., Castro-Ros, A., Pellat, M., Robinson, K., Valter, D., Narang, S., Mishra, G., Yu, A., Zhao, V., Huang, Y., Dai, A., Yu, H., Petrov, S., Chi, E. H., Dean, J., Devlin, J., Roberts, A., Zhou, D., Le, Q. V., and Wei, J. Scaling instruction-finetuned language models. *Journal of Machine Learning Research*, 25(70):1–53, 2024. URL <http://jmlr.org/papers/v25/23-0870.html>.

Comanici, G., Bieber, E., Schaeckermann, M., Pasupat, I., Sachdeva, N., Dhillon, I., Blstein, M., Ram, O., Zhang, D., Rosen, E., et al. Gemini 2.5: Pushing the frontier with advanced reasoning, multimodality, long context, and next generation agentic capabilities. *arXiv preprint arXiv:2507.06261*, 2025.

Doris, A. C., Grandi, D., Tomich, R., Alam, M. F., Ataei, M., Cheong, H., and Ahmed, F. Designqa: A multimodal benchmark for evaluating large language models’ understanding of engineering documentation, 2024. URL <https://arxiv.org/abs/2404.07917>.

Fu, C., Chen, P., Shen, Y., Qin, Y., Zhang, M., Lin, X., Yang, J., Zheng, X., Li, K., Sun, X., Wu, Y., and Ji, R. Mme: A comprehensive evaluation benchmark for multimodal large language models, 2024a. URL <https://arxiv.org/abs/2306.13394>.

Fu, C., Chen, P., Shen, Y., Qin, Y., Zhang, M., Lin, X., Yang, J., Zheng, X., Li, K., Sun, X., Wu, Y., and Ji, R. Mme: A comprehensive evaluation benchmark for multimodal large language models, 2024b. URL <https://arxiv.org/abs/2306.13394>.

Gadre, S. Y., Ilharco, G., Fang, A., Hayase, J., Smyrnis, G., Nguyen, T., Marten, R., Wortsman, M., Ghosh, D., Zhang, J., Orgad, E., Entezari, R., Daras, G., Pratt, S. M., Ramanujan, V., Bitton, Y., Marathe, K., Mussmann, S., Vencu, R., Cherti, M., Krishna, R., Koh, P. W., Saukh, O., Ratner, A., Song, S., Hajishirzi, H., Farhadi, A., Beaumont, R., Oh, S., Dimakis, A., Jitsev, J., Carmon, Y., Shankar, V., and Schmidt, L. Datacomp: In search of the next generation of multimodal datasets. In *Thirty-seventh Conference on Neural Information Processing Systems Datasets and Benchmarks Track*, 2023. URL <https://openreview.net/forum?id=dVaWCDMBof>.

Ging, S., Bravo, M. A., and Brox, T. Open-ended vqa benchmarking of vision-language models by exploiting classification datasets and their semantic hierarchy. *arXiv preprint arXiv:2402.07270*, 2024.

Goyal, Y., Khot, T., Summers-Stay, D., Batra, D., and Parikh, D. Making the V in VQA matter: Elevating the role of image understanding in visual question answering.

In *Proceedings of the IEEE Conference on Computer Vision and Pattern Recognition (CVPR)*, pp. 6904–6913, 2017.

Gupta, T. and Kembhavi, A. Visual programming: Compositional visual reasoning without training. In *2023 IEEE/CVF Conference on Computer Vision and Pattern Recognition (CVPR)*, pp. 14953–14962, 2023. doi: 10.1109/CVPR52729.2023.01436.

Gurari, D., Li, Q., Stangl, A. J., Guo, A., Lin, C., Grauman, K., Luo, J., and Bigham, J. P. VizWiz grand challenge: Answering visual questions from blind people. In *Proceedings of the IEEE Conference on Computer Vision and Pattern Recognition (CVPR)*, pp. 3608–3617, 2018.

Hudson, D. A. and Manning, C. D. GQA: A new dataset for real-world visual reasoning and compositional question answering. In *Proceedings of the IEEE Conference on Computer Vision and Pattern Recognition (CVPR)*, pp. 6700–6709, 2019.

Huggingface. Internvl3-9b, 2025a. URL <https://huggingface.co/OpenGVLab/InternVL3-9B>. Accessed: 2025-09-15.

Huggingface. Qwen2.5-vl-3b-instruct, 2025b. URL <https://huggingface.co/Qwen/Qwen2.5-VL-3B-Instruct>. Accessed: 2025-09-15.

Huggingface. Qwen2.5-vl-3b-instruct-awq, 2025c. URL <https://huggingface.co/Qwen/Qwen2.5-VL-3B-Instruct-AWQ>. Accessed: 2025-09-15.

Huggingface. Qwen2.5-vl-7b-instruct, 2025d. URL <https://huggingface.co/Qwen/Qwen2.5-VL-7B-Instruct>. Accessed: 2025-09-15.

Huggingface. llava-hf/llava-v1.6-34b-hf, 2025e. URL <https://huggingface.co/llava-hf/llava-v1.6-34b-hf>. Accessed: 2026-01-10.

Huggingface. llava-v1.6-mistral-7b-hf, 2025f. URL <https://huggingface.co/llava-hf/llava-v1.6-mistral-7b-hf>. Accessed: 2025-09-15.

Huggingface. llava-v1.6-vicuna-7b-hf, 2025g. URL <https://huggingface.co/llava-hf/llava-v1.6-vicuna-7b-hf>. Accessed: 2025-09-15.

Hurst, A. and OpenAI. Gpt-4o system card. *arXiv preprint arXiv:2410.21276*, 2024. doi: 10.48550/arXiv.2410.21276. URL <https://arxiv.org/abs/2410.21276>. “o” for omni — large multimodal model accepting text, audio, image, and video inputs.

Jiang, Y., Zhang, J., Sun, K., Sourati, Z., Ahrabian, K., Ma, K., Ilievski, F., and Pujara, J. Marvel: Multidimensional abstraction and reasoning through visual evaluation and learning. In Globerson, A., Mackey, L., Belgrave, D., Fan, A., Paquet, U., Tomczak, J., and Zhang, C. (eds.), *Advances in Neural Information Processing Systems*, volume 37, pp. 46567–46592. Curran Associates, Inc., 2024. URL https://proceedings.neurips.cc/paper_files/paper/2024/file/529d8b3a23991e83db07f21727256374-Paper-Datasets_and_Benchmarks_Track.pdf.

Kamath, A., Hessel, J., and Chang, K.-W. What’s up” with vision-language models? investigating their struggle with spatial reasoning. *arXiv preprint arXiv:2310.19785*, 2023.

Khemlani, S., Tran, T., Gyory, N., Harrison, A. M., Lawson, W. E., Thielstrom, R., Thompson, H., Singh, T., and Trafton, J. G. Vision language models are unreliable at trivial spatial cognition. *arXiv preprint arXiv:2504.16061*, 2025.

Li, B., Lin, Z., Peng, W., Nyandwi, J. d. D., Jiang, D., Ma, Z., Khanuja, S., Krishna, R., Neubig, G., and Ramanan, D. Naturalbench: Evaluating vision-language models on natural adversarial samples. *Advances in Neural Information Processing Systems*, 37:17044–17068, 2024a.

Li, C., Wong, C., Zhang, S., Usuyama, N., Liu, H., Yang, J., Naumann, T., Poon, H., and Gao, J. Llava-med: Training a large language-and-vision assistant for biomedicine in one day. In Oh, A., Naumann, T., Globerson, A., Saenko, K., Hardt, M., and Levine, S. (eds.), *Advances in Neural Information Processing Systems*, volume 36, pp. 28541–28564. Curran Associates, Inc., 2023. URL https://proceedings.neurips.cc/paper_files/paper/2023/file/5abcf8ecdacba028c6662789194572-Paper-Datasets_and_Benchmarks.pdf.

Li, H., Jiang, B., Naehu, A., Song, R., Zhang, J., Tjandra-suwita, M., Ekbote, C., Chen, S.-S., Balachandran, A., Dai, W., Chang, R., and Liang, P. P. Puzzleworld: A benchmark for multimodal, open-ended reasoning in puzzlehunts, 2025a. URL <https://arxiv.org/abs/2506.06211>.

Li, J. et al. SEED-Bench: Benchmarking multimodal llms with generative comprehension. *arXiv preprint arXiv:2307.16125*, 2024b.

Li, M., Zhong, J., Chen, T., Lai, Y., and Psounis, K. Eee-bench: A comprehensive multimodal electrical and electronics engineering benchmark, 2025b. URL <https://arxiv.org/abs/2411.01492>.

Liang, C. et al. SCEMQA: Benchmarking scientific and engineering multimodal question answering. *arXiv preprint arXiv:2404.03144*, 2024.

Liu, H., Li, Z., and et al. MMBench: Is your multi-modal model an all-around player? In *Advances in Neural Information Processing Systems (NeurIPS)*, 2023.

Lu, P., Chen, W., Zhu, Y., and et al. Inter-GPS: Interpretable geometry problem solving with formal language and symbolic reasoning. In *Proceedings of the 59th Annual Meeting of the Association for Computational Linguistics (ACL)*, pp. 6774–6786, 2021.

Lu, P., Bansal, H., Xia, T., Liu, J., Li, C., Hajishirzi, H., Cheng, H., Chang, K.-W., Galley, M., and Gao, J. Math-Vista: Evaluating mathematical reasoning of foundation models in visual contexts. In *International Conference on Learning Representations (ICLR)*, 2024a.

Lu, P., Bansal, H., Xia, T., Liu, J., Li, C., Hajishirzi, H., Cheng, H., Chang, K.-W., Galley, M., and Gao, J. Math-vista: Evaluating mathematical reasoning of foundation models in visual contexts. In *The Twelfth International Conference on Learning Representations*, 2024b. URL <https://openreview.net/forum?id=KUNzEQMWU7>.

Lu, P., Bansal, H., Xia, T., Liu, J., Li, C., Hajishirzi, H., Cheng, H., Chang, K.-W., Galley, M., and Gao, J. Mathvista: Evaluating mathematical reasoning of foundation models in visual contexts, 2024c. URL <https://arxiv.org/abs/2310.02255>.

Marino, K., Rastegari, M., Farhadi, A., and Mottaghi, R. Ok-vqa: A visual question answering benchmark requiring external knowledge. In *Proceedings of the IEEE Conference on Computer Vision and Pattern Recognition (CVPR)*, pp. 3195–3204, 2019.

Mathew, M., Karatzas, D., and Jawahar, C. V. DocVQA: A dataset for vqa on document images. In *Proceedings of the IEEE/CVF Winter Conference on Applications of Computer Vision (WACV)*, pp. 2200–2209, 2021.

OpenAI. Hello gpt-4o, 2025a. URL <https://openai.com/index/hello-gpt-4o/>. Accessed: 2025-09-15.

OpenAI. Gpt-4o mini: advancing cost-efficient intelligence, 2025b. URL <https://openai.com/index/gpt-4o-mini-advancing-cost-efficient-intelligence/>. Accessed: 2025-09-15.

OpenAI. Gpt-5.1: A smarter, more conversational chatgpt — openai, 2025c. URL <https://openai.com/index/gpt-5-1/>. Accessed: 2026-01-10.

OpenAI. Introducing gpt-5.2, 2025d. URL <https://openai.com/index/introducing-gpt-5-2/>. Accessed: 2026-01-05.

OpenAI. Introducing openai o3 and o4-mini, 2025e. URL <https://openai.com/index/introducing-o3-and-o4-mini/>. Accessed: 2025-09-15.

OpenAI. Thinking with images, openai, 2025f. URL <https://openai.com/index/thinking-with-images/>. Accessed: 2025-09-15.

OpenAI. Openai o3. <https://openai.com/index/introducing-o3-and-o4-mini/>, 2025. Accessed: 2025-04-16.

Ouyang, L., Wu, J., Jiang, X., Almeida, D., Wainwright, C., Mishkin, P., Zhang, C., Agarwal, S., Slama, K., Ray, A., Schulman, J., Hilton, J., Kelton, F., Miller, L., Simens, M., Askell, A., Welinder, P., Christiano, P. F., Leike, J., and Lowe, R. Training language models to follow instructions with human feedback. In Koyejo, S., Mohamed, S., Agarwal, A., Belgrave, D., Cho, K., and Oh, A. (eds.), *Advances in Neural Information Processing Systems*, volume 35, pp. 27730–27744. Curran Associates, Inc., 2022. URL https://proceedings.neurips.cc/paper_files/paper/2022/file/b1efde53be364a73914f58805a001731-Paper-Conference.pdf.

Pan, C., Yaman, B., Nesti, T., Mallik, A., Allievi, A. G., Velipasalar, S., and Ren, L. Vlp: Vision language planning for autonomous driving. In *Proceedings of the IEEE/CVF Conference on Computer Vision and Pattern Recognition*, pp. 14760–14769, 2024.

Phan, V. M. H., Xie, Y., Qi, Y., Liu, L., Liu, L., Zhang, B., Liao, Z., Wu, Q., To, M.-S., and Verjans, J. W. Decomposing disease descriptions for enhanced pathology detection: A multi-aspect vision-language pre-training framework. In *Proceedings of the IEEE/CVF Conference on Computer Vision and Pattern Recognition (CVPR)*, pp. 11492–11501, June 2024.

Qiao, Y. et al. We-Math: Does your multi-modal llm truly see the diagrams in visual math problems? *arXiv preprint arXiv:2405.18220*, 2024.

Rahmanzadehgervi, P., Bolton, L., Taesiri, M. R., and Nguyen, A. T. Vision language models are blind. In *Proceedings of the Asian Conference on Computer Vision (ACCV)*, pp. 18–34, December 2024.

Saikh, T. and et al. ScienceQA: A multi-choice dataset for science question answering with explanations. In *Empirical Methods in Natural Language Processing (EMNLP)*, 2022.

Schuhmann, C., Beaumont, R., Vencu, R., Gordon, C. W., Wightman, R., Cherti, M., Coombes, T., Katta, A., Mullis, C., Wortsman, M., Schramowski, P., Kundurthy, S. R., Crowson, K., Schmidt, L., Kaczmarczyk, R., and Jitsev, J. LAION-5b: An open large-scale dataset for training next generation image-text models. In *Thirty-sixth Conference on Neural Information Processing Systems Datasets and Benchmarks Track*, 2022. URL <https://openreview.net/forum?id=M3Y74vmsMcY>.

Shao, H., Qian, S., Xiao, H., Song, G., Zong, Z., Wang, L., Liu, Y., and Li, H. Visual cot: Advancing multi-modal language models with a comprehensive dataset and benchmark for chain-of-thought reasoning. In Globerson, A., Mackey, L., Belgrave, D., Fan, A., Paquet, U., Tomczak, J., and Zhang, C. (eds.), *Advances in Neural Information Processing Systems*, volume 37, pp. 8612–8642. Curran Associates, Inc., 2024. URL https://proceedings.neurips.cc/paper_files/paper/2024/file/0ff38d72a2e0aa6dbe42de83a17b2223-Paper-Datasets_and_Benchmarks_Track.pdf.

Singh, A., Natarajan, V., Shah, M., Jiang, Y., Chen, X., Rohrbach, M., Batra, D., and Parikh, D. Towards vqa models that can read. In *Proceedings of the IEEE Conference on Computer Vision and Pattern Recognition (CVPR)*, pp. 8317–8326, 2019.

Surís, D., Menon, S., and Vondrick, C. Vipergpt: Visual inference via python execution for reasoning. In *2023 IEEE/CVF International Conference on Computer Vision (ICCV)*, pp. 11854–11864, 2023. doi: 10.1109/ICCV51070.2023.01092.

Touvron, H., Lavril, T., Izacard, G., Martinet, X., Lachaux, M.-A., Lacroix, T., Rozière, B., Goyal, N., Hambro, E., Azhar, F., et al. Llama: Open and efficient foundation language models. *arXiv preprint arXiv:2302.13971*, 2023.

Vaswani, A., Shazeer, N., Parmar, N., Uszkoreit, J., Jones, L., Gomez, A. N., Kaiser, L. u., and Polosukhin, I. Attention is all you need. In Guyon, I., Luxburg, U. V., Bengio, S., Wallach, H., Fergus, R., Vishwanathan, S., and Garnett, R. (eds.), *Advances in Neural Information Processing Systems*, volume 30. Curran Associates, Inc., 2017. URL https://proceedings.neurips.cc/paper_files/paper/2017/file/3f5ee243547dee91fb0053c1c4a845aa-Paper.pdf.

Wang, J. et al. Charxiv: Chart reasoning benchmark for multimodal llms. *arXiv preprint arXiv:2402.10841*, 2024a.

Wang, K., Pan, J., Shi, W., Lu, Z., Zhan, M., and Li, H. Measuring multimodal mathematical reasoning with math-vision dataset, 2024b. URL <https://arxiv.org/abs/2402.14804>.

Wang, K., Pan, J., Shi, W., Lu, Z., Zhan, M., and Li, H. Measuring multimodal mathematical reasoning with math-vision dataset, 2024c. URL <https://arxiv.org/abs/2402.14804>.

Wang, X., Wei, J., Schuurmans, D., Le, Q. V., Chi, E. H., Narang, S., Chowdhery, A., and Zhou, D. Self-consistency improves chain of thought reasoning in language models. In *The Eleventh International Conference on Learning Representations*, 2023a. URL <https://openreview.net/forum?id=1PL1NIMMrw>.

Wang, Y. et al. SciBench: Benchmarking scientific reasoning in large language models. *arXiv preprint arXiv:2307.10635*, 2023b.

Wei, J., Wang, X., Schuurmans, D., Bosma, M., brian ichter, Xia, F., Chi, E. H., Le, Q. V., and Zhou, D. Chain of thought prompting elicits reasoning in large language models. In Oh, A. H., Agarwal, A., Belgrave, D., and Cho, K. (eds.), *Advances in Neural Information Processing Systems*, 2022. URL https://openreview.net/forum?id=VjQ1MeSB_J.

Yao, S., Yu, D., Zhao, J., Shafran, I., Griffiths, T. L., Cao, Y., and Narasimhan, K. R. Tree of thoughts: Deliberate problem solving with large language models. In *Thirty-seventh Conference on Neural Information Processing Systems*, 2023. URL <https://openreview.net/forum?id=5Xc1ecx01h>.

Yu, W., Yang, Z., Li, L., Wang, J., Lin, K., Liu, Z., Wang, X., and Wang, L. Mm-vet: Evaluating large multimodal models for integrated capabilities. *arXiv preprint arXiv:2308.02490*, 2023.

Yue, X., Ni, Y., Zhang, K., Zheng, T., Liu, R., Zhang, G., Stevens, S., Jiang, D., Ren, W., Sun, Y., Wei, C., Yu, B., Yuan, R., Sun, R., Yin, M., Zheng, B., Yang, Z., Liu, Y., Huang, W., Sun, H., Su, Y., and Chen, W. Mmmu: A massive multi-discipline multimodal understanding and reasoning benchmark for expert agi, 2024a. URL <https://arxiv.org/abs/2311.16502>.

Yue, X., Zheng, T., Ni, Y., Wang, Y., Zhang, K., Tong, S., Sun, Y., Yu, B., Zhang, G., Sun, H., Su, Y., Chen, W., and Neubig, G. Mmmu-pro: A more robust multi-discipline multimodal understanding benchmark, 2025. URL <https://arxiv.org/abs/2409.02813>.

Yue, X. et al. MMMU: A massive multi-discipline multimodal understanding and reasoning benchmark. *arXiv preprint arXiv:2311.16502*, 2024b.

Zhang, C., Gao, F., Jia, B., Zhu, Y., and Zhu, S.-C. Raven: A dataset for relational and analogical visual reasoning. In *2019 IEEE/CVF Conference on Computer Vision and Pattern Recognition (CVPR)*, pp. 5312–5322, 2019. doi: 10.1109/CVPR.2019.00546.

Zhang, R., Jiang, D., Zhang, Y., Lin, H., Guo, Z., Qiu, P., Zhou, A., Lu, P., Chang, K.-W., Gao, P., and Li, H. MathVerse: Does your multi-modal LLM truly see the diagrams in visual math problems? *arXiv preprint arXiv:2403.14624*, 2024a.

Zhang, W., Ng, W. E., Ma, L., Wang, Y., Zhao, J., Koencke, A., Li, B., and Wang, L. Sphere: Unveiling spatial blind spots in vision-language models through hierarchical evaluation. *arXiv preprint arXiv:2412.12693*, 2024b.

Zhang, W., Zhou, Z., Zheng, Z., Gao, C., Cui, J., Li, Y., Chen, X., and Zhang, X.-P. Open3dvqa: A benchmark for comprehensive spatial reasoning with multimodal large language model in open space. *arXiv preprint arXiv:2503.11094*, 2025a.

Zhang, Z., Chen, Z., Zhang, Z., Sun, Y., Tian, Y., Jia, Z., Li, C., Liu, X., Min, X., and Zhai, G. Puzzlebench: A fully dynamic evaluation framework for large multimodal models on puzzle solving, 2025b. URL <https://arxiv.org/abs/2504.10885>.

Appendix

A. Diagnostic Probe Example

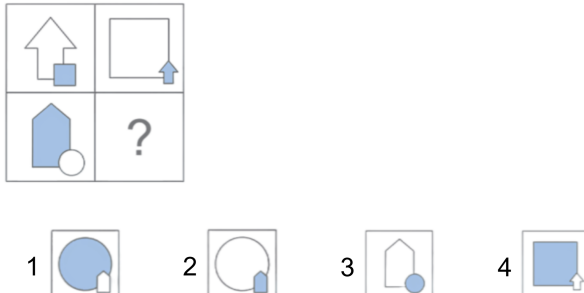


Figure 2. Sample VRIQ example with corresponding probe questions

This example demonstrates our hierarchical annotation framework applied to a 2×2 matrix reasoning puzzle. We design targeted probes that systematically isolate different task-relevant perceptual and reasoning attributes required to solve this puzzle.

Perceptual Probes

These verify accurate perception of individual visual elements without requiring pattern recognition:

Shape Dimension:

- Q: “In the top-left panel, what is the small shape located inside the larger shape?”
→ Expected: *square*
- Q: “In the bottom-left panel, what is the small shape?”
→ Expected: *circle*

Position Dimension:

- Q: “In the top-right panel, is the arrow the large or the small shape?”
→ Expected: *small*
- Q: “In option 2, is the circle the large shape or the small shape?”
→ Expected: *large*

Detail Dimension:

- Q: “In the top-left panel, is the large shape a solid color or an outline?”
→ Expected: *outline*
- Q: “In the bottom-left panel, is the large shape a solid color or an outline?”
→ Expected: *solid*

Reasoning Probes

These probes remove visual input and supply all task-relevant facts in text:

- Q: “Given a matrix where top-left has a large outline arrow with small filled square, top-right has large outline rectangle with small filled arrow, and bottom-left has large filled pentagon with small outline circle—would bottom-right have a small outline pentagon?”
→ Expected: *yes*
- Q: “Given the same matrix setup, would bottom-right have a large outline circle?”
→ Expected: *no*

B. Procedure for Natural Question Generation

We leverage a semi-agentic procedure to generate natural examples. Specifically, we first generate 5 examples per category by a human. Then, we use these questions as few-shot examples and task the GPT-5.2-Thinking model to generate additional novel ideas for each task; to ensure diversity and consistency, we first ask it to propose 15 potential categories for each task and then propose 20 specific examples for each category. To ensure correctness and high quality, we employed 5 PhD students to manually rank the feasibility of the proposed categories and examples. We then filter for the top 10 categories and the top 10 examples by overall rank (votes), leaving 100 total natural examples for each task. We ask the same group of students to search for appropriate natural image examples following the proposed idea, in compliance with copyright laws. For example, for the task “odd one out”, the generated 15 categories may include *biology, physics, rotation, etc.*; for biology, one of such 20 novel ideas may be, as the given sequence *frog egg, tadpole, tadpole with legs*, and as the options *a frog egg, adult frog, a fish, a lizard* with adult frog as the correct answer; the student group would then search for appropriate publicly available and allowed images and arrange them to create the final example for benchmark purposes.

C. Abstract Puzzle Sourcing and Modification

C.1. Source Materials and Selection Criteria

The abstract-domain puzzles in VRIQ were built primarily from **national civil-service and standardized aptitude exam materials** obtained from **publicly accessible sources**.

We applied a **manual screening process** to ensure suitability and quality. In particular, we removed items that (i) relied on textual content, (ii) contained ambiguous or non-unique answers, (iii) were visually low-resolution or poorly legible, or (iv) did not match our target task formats. All retained puzzles were verified by human reviewers to ensure the underlying rule is well-defined and solvable.

C.2. Reformatting and Modification Procedure

Many sourced exam items appear in heterogeneous layouts (e.g., differing panel arrangements, answer-option formatting, or inconsistent visual styles). To standardize the benchmark, we **reconstructed** each selected puzzle into a unified VRIQ template:

- Panels were **segmented** (when necessary) and **reassembled** into the canonical task configuration for the corresponding category.
- Answer options were **normalized** to a consistent multiple-choice format (with a fixed option layout and consistent rendering).
- When minor artifacts (e.g., misalignment, faint scan marks) interfered with readability, we performed **light cleanup** while preserving the original reasoning rule.

To reduce duplication and improve robustness, a subset of sourced puzzles were **modified into novel instances** by altering superficial visual attributes (e.g., shape identities, counts, orientations, or styling) while keeping the **same underlying rule structure**. These modifications were designed to preserve psychometric intent while decreasing the likelihood of direct memorization from commonly circulated copies.

C.3. Manually Authored Abstract Items

In addition to sourced exam items, we also included a set of **manually authored abstract puzzles** created by the authors. These items were designed to (i) increase coverage of underrepresented rule types, (ii) balance category difficulty, and (iii) expand the diversity of perceptual demands (e.g., count, position, rotation/orientation, symmetry/pattern, distractor similarity).

Manual items were created by following the same category definitions and then drawing new shapes and panel contents from scratch to instantiate the intended rule. All manually authored puzzles underwent the same quality-control pipeline as sourced items, including independent solving and answer verification.

C.4. Temporal Scope

Puzzle selection, reconstruction, manual authoring, and validation were conducted between **May 2025 and January 2026**.

C.5. Quality Control and Answer Verification

To ensure correctness and eliminate ambiguity, each abstract puzzle was independently solved by two reviewers. Items were accepted only if the reviewers agreed on a **single correct answer** and confirmed that distractors were plausible yet incorrect under the intended rule. Disagreements or multiple-valid-answer cases were revised or removed.

D. o3 Tool-Use Examples

We provide three representative examples demonstrating how tool-augmented reasoning performs across different task categories and failure modes.

D.1. Example 1: Figure Rotation (Abstract Domain - Success)

Task. Identify the next image in the sequence of compass orientations shown in Figure 3.

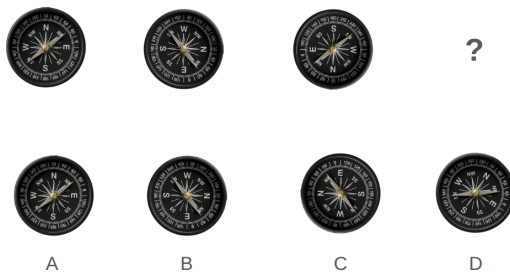


Figure 3. Input sequence with the missing final image and multiple-choice options (A–D).

Tool call sequence (logged):

1. `crop(x=40, y=20, w=240, h=240)` % first compass
2. `crop(x=320, y=20, w=240, h=240)` % second compass
3. `crop(x=600, y=20, w=240, h=240)` % third compass
4. `rotate(angle=90)` % applied to first compass
5. `rotate(angle=180)` % applied to first compass
6. `rotate(angle=270)` % applied to first compass

o3 Response

The pattern is brutally simple:

Each compass rotates 90° clockwise each step: 1st has N on top → 2nd has W on top → 3rd has S on top → next must have E on top.



Figure 4. Reference image after 270° rotation produced by the tool, used for comparison with the answer options.

Also, the missing wedge on the left grows each step, so the next one should still have that left-side cut.

Only Option C matches (E at the top + left-side cut).

Answer: C

Predicted answer: C (correct) **Ground truth:** C

Why tools help. Instead of estimating rotation from raw pixels, o3 explicitly generates a rotated reference (Figure 4) and compares it against candidate options. This converts a challenging rotation perception task (52.4% failure rate, Table 4) into direct visual alignment, demonstrating how tools can successfully mitigate certain perceptual bottlenecks.

D.2. Example 2: Sequence Completion with Counting Errors (Natural Domain)

Task. Predict the next image in the log-stacking sequence shown in Figure 5.

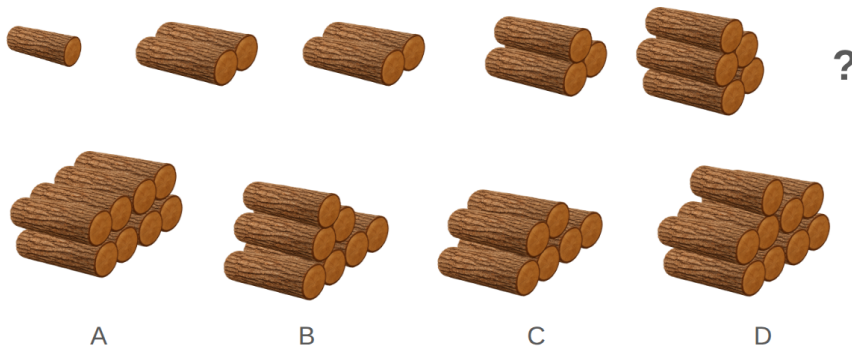


Figure 5. Natural-domain sequence completion task with missing final image and answer options (A–D).

Tool call sequence (logged):

1. crop(...) % isolate sequence region
2. crop(...) % option A
3. crop(...) % option B
4. crop(...) % option C
5. crop(...) % option D

o3 Response

Count the logs in the top sequence:
1st: 1

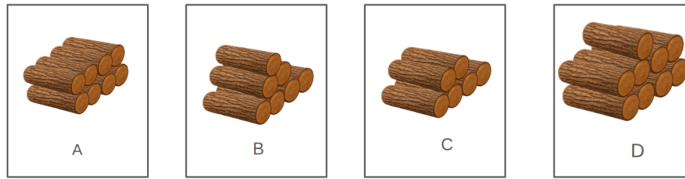


Figure 6. Cropped candidate options used by o3 for visual inspection and counting.

2nd: 2
 3rd: 2 (same total, just arranged slightly differently)
 4th: 3
 5th: 5
 That's the Fibonacci pattern starting as 1, 2, 2, 3, 5, so the next should be 8 logs.
 Among the options, only D shows a stable stack of 8 logs (arranged as 3 + 3 + 2).
 Answer: D

Predicted answer: D (incorrect) **Ground truth:** A

Failure analysis. The tool trace reveals o3 correctly inferred that the sequence follows a Fibonacci-like pattern and predicted the next configuration should contain eight logs. However, after isolating the answer options (Figure 6), the model miscounted logs in the rendered stacks due to occlusion and overlapping cylindrical structures, incorrectly selecting Option D.

This demonstrates that tool-assisted isolation improves pattern reasoning but does not resolve fine-grained counting in cluttered natural scenes—consistent with counting having the highest failure rate (73.8%, Table 4).

D.3. Example 3: Matrix Reasoning with Persistent Errors (Abstract Domain)

Task. Predict the missing cell in a 3×3 matrix of circle patterns (Figure 7).

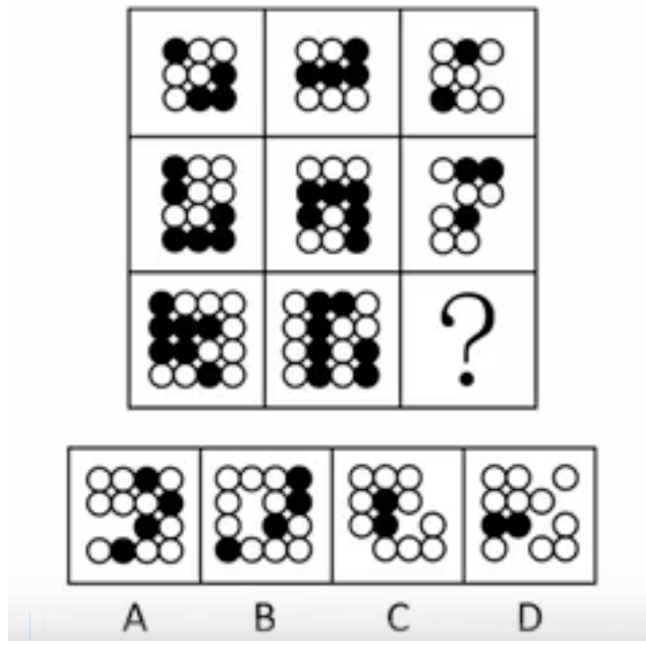


Figure 7. Abstract matrix reasoning task with one missing cell (bottom-right).

Tool execution summary. Over 352 seconds, the model performed:

- 13 cropping operations (matrix cells and answer options)
- 8 circle-detection attempts using HoughCircles with varying parameters
- Position clustering to classify black vs. white circles

What went right. The model correctly identified progressive grid size increases ($3 \times 3 \rightarrow 4 \times 3 \rightarrow 5 \times 4$), demonstrating successful structural pattern recognition.

What went wrong. Despite extensive tool use, perception errors persisted:

- Options A & B: 14 circles detected (4 black, 10 white)
- Options C & D: 11 circles detected (1 black, 10 white)
- Cell (Row 1, Col 3): only 5 circles detected (undercount)
- Cell (Row 2, Col 3): 9 circles detected

These miscounts corrupted the final decision. Additionally, the model failed to detect the actual transformation rule: circles that are black in *both* columns 1 and 2 should be removed in column 3.

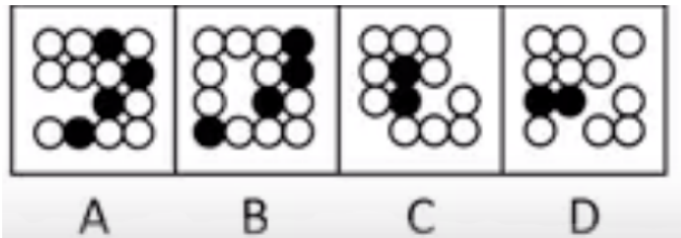


Figure 8. Tool execution trace showing repeated circle-detection attempts. Despite systematic cropping, accurate enumeration and spatial localization remain unreliable under clutter.

o3 Response

A. Because in the rightmost column, the black circles keep the same ‘‘top-right pair’’ pattern from row 1 \rightarrow row 2, and in row 3 that pattern expands into the larger layout in the only way that stays consistent with the build-up seen in the first two columns. Option A matches that continuation; the others either drop required blacks or place them where the progression never puts them.

Predicted answer: A (incorrect) **Ground truth:** B

Key takeaway. Tool augmentation enabled correct structural reasoning but failed to resolve counting (73.8% failure) and position (58.2% failure) bottlenecks (Table 4). This confirms that tools improve reasoning strategies but do not eliminate fundamental perception limitations in abstract visual tasks.

D.4. Summary

These examples illustrate that tool-augmented reasoning provides:

- **Successful bypass of some perception bottlenecks:** Rotation tasks benefit significantly from programmatic transformations (Example 1).

- **Improved reasoning but some perception errors:** Pattern recognition improves, but enumeration in cluttered scenes remains unreliable (Examples 2–3).
- **Necessary but not sufficient improvement:** Tools eliminate many reasoning failures but cannot fully overcome fundamental perception limitations, explaining why o3 did not achieve 100% performance across all categories.

E. Natural Dataset Samples



Figure 9. Sample VRIQ natural Sequence Completion questions



Which option in the second row correctly depicts the image in the first row rotated clockwise for 180 degrees?



A



Which option in the second row correctly depicts the image in the first row rotated clockwise for 270 degrees?



A



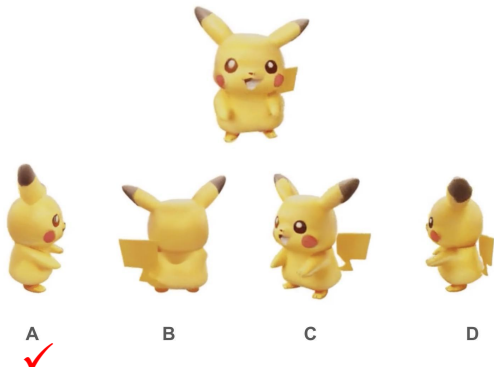
Which option in the second row correctly depicts the image in the first row rotated clockwise for 270 degrees?



A



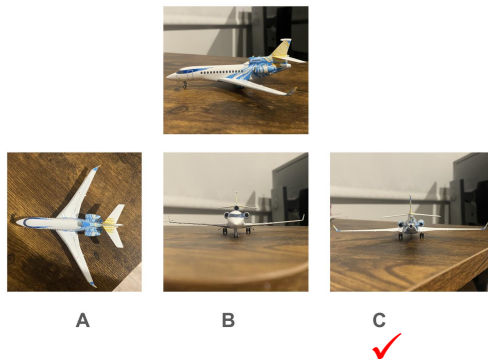
Figure 10. Sample VRIQ natural Rotation questions



Which option in the second row correctly depicts the left view of the image in the first row?



Which option in the second row correctly depicts the back view of the image in the first row?



Which option in the second row correctly depicts the right view of the image in the first row?

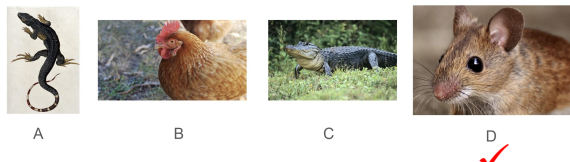
Figure 11. Sample VRIQ natural 3D questions



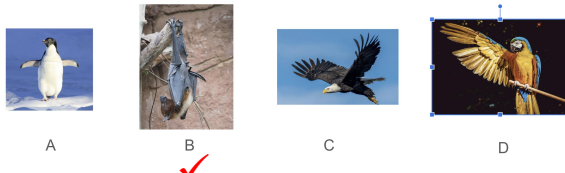
✓



✓



✓



✓

Figure 12. Sample VRIQ natural Odd One Out questions

Which option below continues the sequence?

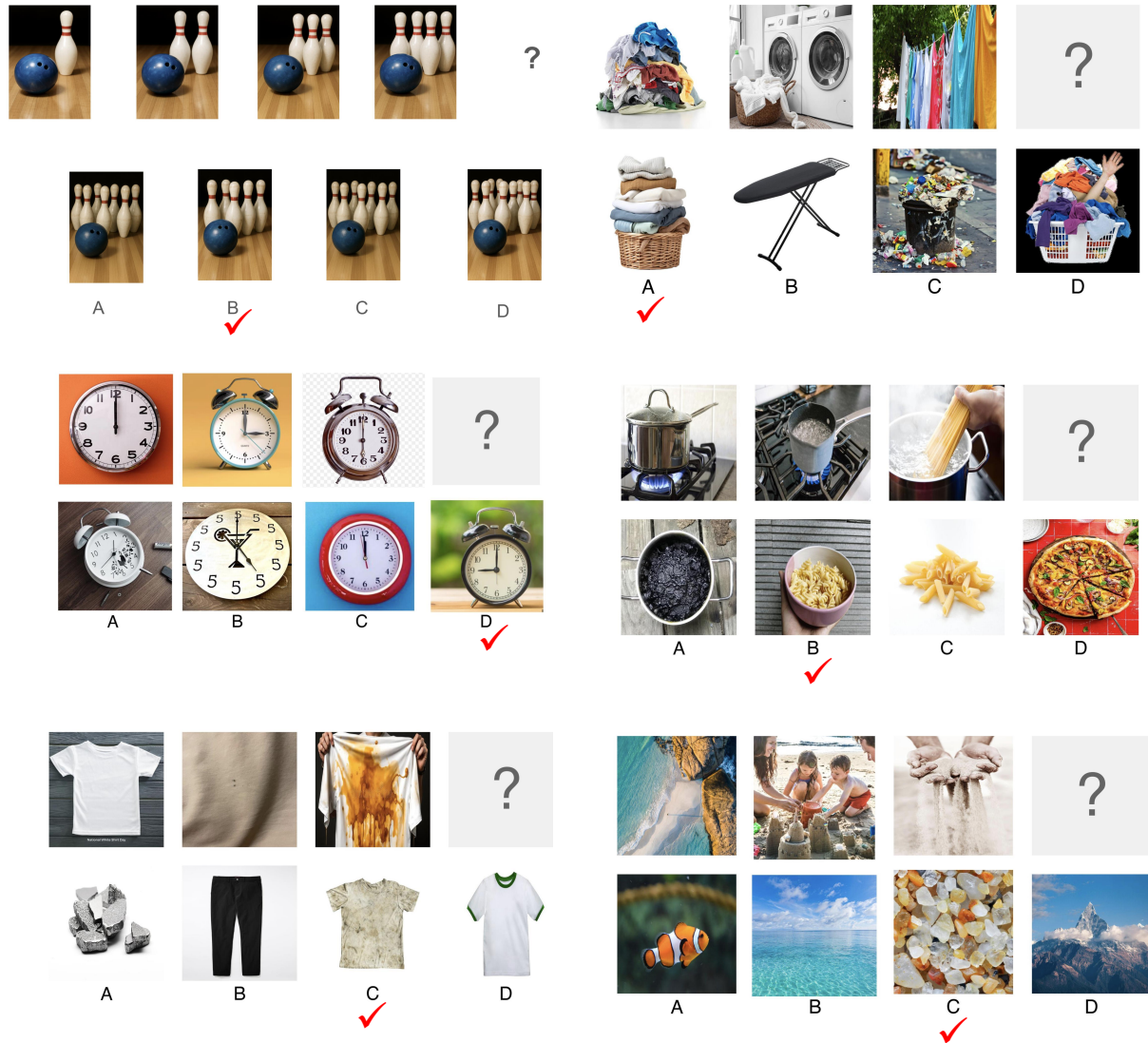


Figure 13. More VRIQ natural Sequence Completion questions